SLAC-PUB-12920

Studies of $\tau^- \to h^- h^- h^+ \nu$ and $\tau^- \to K^- \pi^0 \nu$ Decays at *BABAR*

I. M. Nugent[a*] (representing the *BABAR* Collaboration)

[a]Department of Physics and Astronomy, University of Victoria,
PO Box 3055, STN CSC, Victoria, BC, V8W 3P6 Canada

We present preliminary inclusive branching fraction measurements of $\tau^- \to h^- h^- h^+ \nu$ ($h = \pi$ or K) and $\tau^- \to K^- \pi^0 \nu$ decay modes using a sample of τ-pair events collected by the *BABAR* detector at the SLAC PEP-II asymmetric e^+e^- storage ring. The branching fractions of $\tau^- \to \pi^-\pi^-\pi^+\nu$, $\tau^- \to K^-\pi^-\pi^+\nu$ and $\tau^- \to K^-\pi^-K^+\nu$ are measured with higher precision than previously published results and the inclusive branching fraction $\tau^- \to K^-K^-K^+\nu$ is measured for the first time. In addition, the first measurement of the branching fraction $\tau^- \to \pi^-\phi\nu$ and the measurement of the branching fraction $\tau^- \to K^-\phi\nu$ are determined by means of a binned maximum likelihood fit to the K^+K^- invariant mass distribution. These branching fractions are extracted by means of a migration matrix that accounts for the cross contamination between the $\tau \to h^- h^- h^+ \nu$ modes. The preliminary $\tau^- \to K^-\pi^0\nu$ branching fraction and invariant mass distributions are also presented in this paper.

1. Introduction

Hadronic decays of the τ lepton provide a unique opportunity to probe the coupling of the weak current to the first and second generations of quarks with unprecedented precision[1]. For τ decays with unity strangeness (in other words, there is an odd number of kaons in the final state), the CKM matrix element $|V_{us}|$ and the strange quark mass m_s can be extracted with the spectral density function via Finite Energy Sum Rules [2–6]. The measurement of the strange spectral density function is currently the limiting factor in the extraction of the two fundamental parameters of the Standard Model (SM) from τ decays, especially in the high invariant mass region where the theoretical uncertainties can be mitigated. $\tau^- \to K^-\pi^0\nu$ is one of the dominant channels in the strange spectral density function and, therefore, the minimization of its uncertainty is required. Currently, one of the dominant experimental uncertainties in the strange spectral density function arises from the uncertainty on $\mathcal{B}(\tau^- \to K^-\pi^-\pi^+\nu)$. The decay $\tau^- \to K^-K^-K^+\nu$ contributes to the high invariant mass region where precise information is lacking. The $\mathcal{B}(\tau^- \to \pi^-\phi\nu)$ is useful in understanding the mixing of the $\omega-\phi$ and the violation of the OZI Rule [7]. There has also been some theoretical interest in $\tau^- \to K^-\pi^-K^+\nu$ because of the Wess-Zumino anomaly [8,9].

*We are grateful for the extraordinary contributions of our PEP-II colleagues in achieving the excellent luminosity and machine conditions that have made this work possible. The success of this project also relies critically on the expertise and dedication of the computing organizations that support *BABAR*. The collaborating institutions wish to thank SLAC for its support and the kind hospitality extended to them. This work is supported by the US Department of Energy and National Science Foundation, the Natural Sciences and Engineering Research Council (Canada), Institute of High Energy Physics (China), the Commissariat à l'Energie Atomique and Institut National de Physique Nucléaire et de Physique des Particules (France), the Bundesministerium für Bildung und Forschung and Deutsche Forschungsgemeinschaft (Germany), the Istituto Nazionale di Fisica Nucleare (Italy), the Foundation for Fundamental Research on Matter (The Netherlands), the Research Council of Norway, the Ministry of Science and Technology of the Russian Federation, and the Particle Physics and Astronomy Research Council (United Kingdom). Individuals have received support from CONACyT (Mexico), the A. P. Sloan Foundation, the Research Corporation, and the Alexander von Humboldt Foundation.

Contributed to 9th International Workshop on Tau Lepton Physics (Tau06), 09/19/2006--9/22/2006, Pisa, Italy

Work supported in part by US Department of Energy contract DE-AC02-76SF00515

2. The *BABAR* Detector, Dataset, and Monte Carlo Samples

The data sets employed in this analysis were collected with the *BABAR* detector at the PEP-II storage ring at a centre-of-mass (CM) energy near $\sqrt{s} = 10.58$GeV where the cross section is $\sigma(\tau^+\tau^-) = 0.89 \pm 0.02$[12]. The $\tau \to h^-h^-h^+\nu$ analysis uses a data set with a luminosity of $\mathcal{L} = 344fb^{-1}$, while the $\tau^- \to K^-\pi^0\nu$ analysis uses a slightly smaller data set with a luminosity of $\mathcal{L} = 230fb^{-1}$. The $e^+e^- \to \tau^+\tau^+$ events are simulated with the KK2F [13] Monte Carlo (MC) generator, which include higher order corrections, and the τ decays are simulated with the measured rates [11] using Tauola [14]. GEANT4 [15] is used to simulate the detector response. The simulated MC and data events are then reconstructed in the same manner [12–14,16,17].

The *BABAR* detector is described in detail elsewhere [10]. Charged-particle (track) momenta are measured with a 5-layer double-sided silicon vertex tracker and a 40-layer drift chamber inside a 1.5-T superconducting solenoidal magnet. An electromagnetic calorimeter consisting of 6580 CsI(Tl) crystals is used to identify electrons and photons, a ring-imaging Cherenkov detector is used to identify charged hadrons, and the instrumented magnetic flux return (IFR) is used to identify muons. Particle attributes are reconstructed in the laboratory frame and then boosted to the e^+e^- CM frame using the measured asymmetric beam energies.

3. Analysis Strategy

The $\tau^- \to h^-h^-h^+\nu$ (charge conjugation is implied throughout this paper) analysis selected a pure sample of $e^+e^- \to \tau^+\tau^-$ pairs, where the signal side contains 3 hadrons and the partner τ^+ decays leptonically ($\tau \to l\nu\bar{\nu}$ where $l = e$ or μ). The $h^\pm$ are then identified as either kaon or pions and the decay is classified as: $\tau^- \to \pi^-\pi^-\pi^+\nu$, $\tau^- \to K^-\pi^-\pi^+\nu$, $\tau^- \to K^-\pi^-K^+\nu$, or $\tau^- \to K^-K^-K^+\nu$. An efficiency migration matrix that takes into account $\pi \leftrightarrow K$ cross contaminations is determined from the MC and utilized to extract the number of signal events.

$$\mathbf{N}_j^{Sig} = \sum_i (\epsilon^{-1})_{ji} \left(\mathbf{N}_i^{Data} - \mathbf{N}_i^{Bkg} \right) \quad (1)$$

where $\mathbf{N}_j^{Sig}$ is the number of signal events, $\mathbf{N}_i^{Data}$ is the number of selected data events, $\mathbf{N}_i^{Bkg}$ is the number of MC background events selected, ϵ_{ij} is the efficiency matrix determined from MC, i is the selected 3 prong mode index, and j is the true 3 prong mode index. The MC-data differences in the simulation of the MC particle identification are corrected by using data control samples for pions and kaons from $D^{*+} \to \pi^+D^0$, $D^0 \to \pi^+K^-$. The branching fraction is then determined from

$$\mathbf{Br}_j = \frac{1}{2\mathcal{L}\sigma_{\tau^+\tau^-}} \frac{\mathbf{N}_j^{Sig}}{\epsilon_{Pre,j}} \quad (2)$$

where $\mathcal{L}$ is the luminosity, $\sigma_{\tau^+\tau^-}$ is the $e^+e^- \to \tau^+\tau^-$ cross section, and $\epsilon_{Pre,j}$ is the efficiency for the preselection, including the trigger, not included in the efficiency migration matrix.

The branching fraction of the $\tau^- \to \pi^-\phi\nu$ and $\tau^- \to K^-\phi\nu$ are measured by fitting the background subtracted K^+K^- invariant mass distributions for these decays, and then using the efficiency migration matrix to account for cross feed between the two channels.

As with the $\tau \to h^-h^-h^+\nu$ analysis, the $\tau \to K^-\pi^0\nu$ analysis selects a pure sample of $e^+e^- \to \tau^+\tau^-$ pairs, where the partner τ^+ decays leptonically. The signal side is, however, required to contain a kaon and a π^0. Once the $\tau^- \to K^-\pi^0\nu$ are selected, the branching fraction is determined from

$$\mathbf{Br}_{\tau\to K^-\pi^0\nu} = \frac{N^{Sel} - N^{Bkg}}{2\mathcal{L}\sigma_{\tau^+\tau^-}\epsilon_{\tau\to K^-\pi^0\nu}} \quad (3)$$

where N^{Sel} is the number of selected data events, N^{Bkg} is the number of MC background events selected, and $\epsilon_{\tau\to K^-\pi^0\nu}$ is the total selection efficiency for the $\tau \to K^-\pi^0\nu$ determined from MC.

Table 1
The particle identification component of the efficiency migration matrix represented in percentages.

Candidates	Decay Modes (Truth)			
	$\pi^-\pi^-\pi^+$	$K^-\pi^-\pi^+$	$K^-\pi^-K^+$	$K^-K^-K^+$
$\pi^-\pi^-\pi^+$	97.68%	22.81%	4.79%	1.02%
$K^-\pi^-\pi^+$	1.42%	74.72%	16.29%	6.50%
$K^-\pi^-K^+$	0.01%	0.52%	60.08%	25.78%
$K^-K^-K^+$			0.27%	50.72%

4. Event Selection and Analysis

4.1. $\tau^- \to h^-h^-h^+\nu$

The event selection of $\tau \to h^-h^-h^+\nu$ begins with the identification of events with four well reconstructed tracks, which do not originate from conversions in the material of the detectors, and have a net charge of zero. The tracks in the event are required to be within the geometric acceptance of the DIRC and the EMC. Furthermore, the track must have a minimum transverse momentum of 250MeV, enabling them to reach the DIRC for particle identification. Because τ pairs are produced back-to-back, it is convenient to select them by splitting the event into two hemispheres in the CM frame, with the plane orthogonal to the thrust axis where the thrust has been determined from all of the reconstructed tracks and neutrals in the event. The "tag hemisphere" is required to have one isolated track that is identified as either an electron or a muon. To reduce the non-τ background, the neutral energy in the tag hemisphere measured by the EMC, which is not associated with the electron (muon) track, must be below 1.0(0.5)GeV. The event shape is also used to discriminate against the $q\bar{q}$ background and two photon events. The event is required to have a high thrust to reject $q\bar{q}$ events; and the scaled CM transverse momentum of the event, the momentum orthogonal to the beam axis, is required to be greater than 0.9% of the centre of mass energy. This missing momentum implies that there is one or more undetected particles. This reduces the $e^+e^- \to q\bar{q}$ background to $\sim 0.1\%$. To remove contamination from Bhabha and $e^+e^- \to \mu^+\mu^-$, in which an undetected photon converts into an e^+e^- pair, the decay side tracks must fail the electron identification algorithm and the tag track is required to have a maximum momentum of less than 80% of $\sqrt{s}/2$.

The remaining backgrounds are primarily from τ decays with π^0 and K^0_S. Identified pairs of oppositely charged tracks which have a mass consistent with being that of the K^0_S are removed, if the vertex of the track pair is more than six standard deviations from the interaction point. τ background with π^0 are removed by vetoing events with one or more reconstructed π^0's and by requiring that energy in the decay hemisphere, which is deposited in the EMC and is not associated with a charge particle, is less than 200MeV.

Once the events have been selected, the signal tracks are then identified as either a kaon or a pion using a likelihood approach with the Cherenkov angle from the DIRC and the dE/dx from the DCH and SVT. An event is classified as $\tau^- \to \pi^-\pi^-\pi^+\nu$ if all three hadron tracks are identified as pions. If there are two oppositely charged pions and one kaon, the event is classified as $K^-\pi^-\pi^+$; if there are two oppositely charged kaons and one pion, the event is classified as $K^-\pi^-K^+$. Lastly, if all the hadrons are classified as kaons, the event is selected as $K^-K^-K^+$.

The characteristic efficiency (excluding the particle identification and cross feed), the branching fraction determined from equation 1 and 2, and, for comparison, the PDG branching fractions are presented in table 2. The efficiency variation between the four decay channels is primarily due to transverse momentum cut and the K^0_S veto.

The systematic uncertainties for this analysis include: the luminosity and cross section determined with KK2F; the migration matrix statis-

Table 2
The characteristic selection, efficiencies excluding particle identification, and the branching fraction determined using equations 1 and 2 where, the uncertainties are statistical and systematic respectively. For comparison, the world averages from the PDG are shown in the bottom row.

	$\pi^-\pi^-\pi^+$	$K^-\pi^-\pi^+$
ϵ	2.8%	3.2%
BR	$(9.11 \pm 0.01 \pm 0.26) \times 10^{-2}$	$(2.88 \pm 0.02 \pm 0.11) \times 10^{-3}$
Br_{PDG}	$(9.02 \pm 0.08) \times 10^{-2}$	$(3.33 \pm 0.35) \times 10^{-3}$

	$K^-\pi^-K^+$	$K^-K^-K^+$
ϵ	3.5%	3.9%
Br	$(1.371 \pm 0.011 \pm 0.040) \times 10^{-3}$	$(1.59 \pm 0.14 \pm 0.11) \times 10^{-5}$
Br_{PDG}	$(1.53 \pm 0.10) \times 10^{-3}$	$(3.7) \times 10^{-5}$@90%CL

The PDG branching fractions are given in ref. [11].

Table 3
The major components of the systematic uncertainties for $\tau \to h^-h^-h^+\nu$ expressed in percentages.

Systematic	$\pi^-\pi^-\pi^+$	$K^-\pi^-\pi^+$	$K^-\pi^-K^+$	$K^-K^-K^+$
$\mathcal{L}\sigma_{e^+e^-\to\tau^+\tau^-}$	2.4%	2.4%	2.4%	2.4%
MC stat & PID	0.4%	2.5%	0.8%	4.4%
Kinematics	1.2%	1.1%	0.9%	4.0%
EMC & DCH	0.8%	0.8%	0.8%	1.2%
Trigger	0.1%	0.1%	0.1%	0.1%
Backgrounds	0.4%	1.4%	0.4%	2.5%
Total	2.9%	3.8%	2.8%	6.9%

The significance of $\tau^- \to K^-K^-K^+\nu$ is 8.9σ.

tics uncertainty contributing to the efficiency, combined with the particle identification uncertainty determined from the wrong sign combinations and data control samples; the kinematic modelling of the decay; the uncertainty due to the EMC tracking scale and resolution, combined with the sensitivity of the measurements to hadronic and electromagnetic modelling in the EMC; the modelling uncertainty of the trigger; and the uncertainty of the background modelling for the subtraction of τ and non-τ backgrounds. These uncertainties are summarized in table 3 with the total uncertainty.

4.2. The fitting of $\pi^-\phi$ and $K^-\phi$.

In figures 1 and 2, a $\phi(1020)$ resonance is evident in both the $\tau^- \to K^-\pi^-K^+\nu$ and $\tau^- \to K^-K^-K^+\nu$ decay modes. To increase the signal-to-background, both of these samples are enhanced by loosening the kaon selection criteria. The contributions from τ and non-τ backgrounds are subtracted from the K^-K^+ invariant mass distribution for $K^-\pi^-K^+$ and $K^-K^-K^+$ channels. The $\phi(1020)$ peak in the K^-K^+ invariant mass distribution for the $K^-\pi^-K^+$ channel is fitted with a binned maximum likelihood to extract the number of measured data events, where the ϕ peak is modelled by a Breit-Wigner convoluted with a Gaussian and the $K^-\pi^-K^+$ background is modelled with a polynomial of 3rd order. The

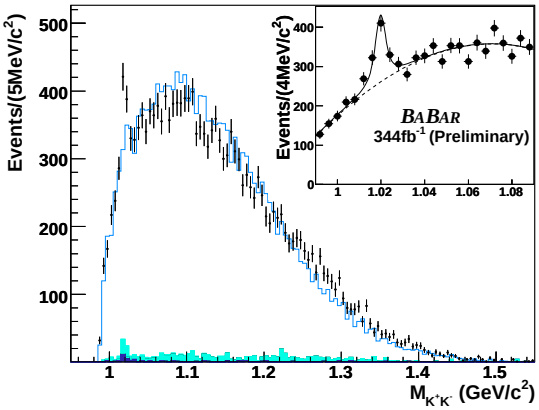

Figure 1. The invariant mass distribution for the K^+K^- pair in the $\tau^- \to K^-\pi^-K^+\nu$ decay. The dots represent the data; the open histogram represents the $\tau^- \to K^-\pi^-K^+\nu$ MC; the light-shaded histogram represents MC cross feed; and the dark-shaded histogram represents the MC background. The insert presents the results of the fit to the data set with the loosened kaon selector as discussed in the text. In the fit, the cross feed and background have been subtracted. The solid line represents the total fit and the dashed line represents the background component of the fit. The MC in both the distribution and the fit are luminosity normalized to the measured $\tau^- \to K^-\pi^-K^+\nu$ branching fraction.

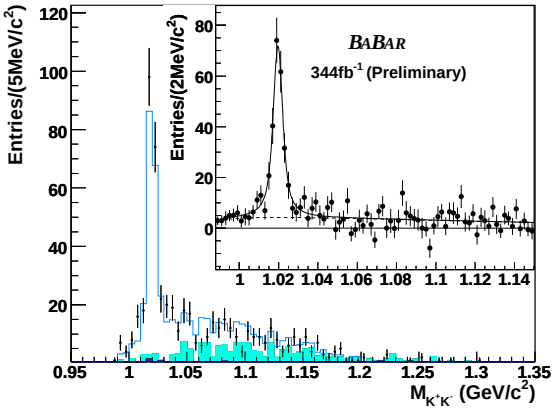

Figure 2. The invariant mass distribution for the K^+K^- pair in the $\tau^- \to K^-K^-K^+\nu$ decay with both pairs from each event. The dots represent the data; the open histogram represents the $\tau^- \to K^-K^-K^+\nu$ MC; the light-shaded histogram represents MC cross feed; and the dark-shaded histogram represents the MC background. The insert presents the results of the fit to the data set with the loosened kaon selector as discussed in the text. In the fit, the cross feed and background have been subtracted. The solid line represents the total fit and the dashed line represents the background component of the fit. The MC in both the distribution and the fit are luminosity normalized to the measured $\tau^- \to K^-K^-K^+\nu$ branching fraction.

shape of the $K^-\pi^-K^+$ background is varied within the uncertainty to yield $< 1\%$ systematic uncertainty. Similarly, the number of measured data events for the $K^-K^-K^+$ decay mode is extracted with a binned maximum likelihood, from the K^-K^+ invariant mass distribution with both combinations of K^-K^+ included. The signal is modelled with a Breit-Wigner convoluted with a Gaussian, while the combinatoric background is modelled with an "Argus-like" function [18]. For both the $K^-\pi^-K^+$ and the $K^-K^-K^+$ fits, the σ for the Gaussian, which describes the detector resolution, is fixed to a value determined from fitting the MC signal, 1.28MeV. Using equations 1 and 2, with the efficiency matrix corresponding to the looser kaon selector the $\tau^- \to \pi^-\phi\nu$ and $\tau^- \to K^-\phi\nu$ branching fractions are determined to be $(3.49\pm0.55\pm0.32)\times10^{-5}$ with a significance 5.5σ and $(3.48\pm0.20\pm0.26)\times10^{-5}$ with a significance of 10.6σ. Furthermore, the $\tau^- \to K^-\phi\nu$ fit indicates that the $\tau^- \to K^-K^-K^+\nu$ decay is saturated by the $\tau^- \to K^-\phi\nu$ channel.

4.3. $\tau^- \to K^-\pi^0\nu$

In the $\tau^- \to K^-\pi^0\nu$ analysis, the events are divided into two hemispheres by the plane perpendicular thrust axis. Each hemisphere is required to have one well reconstructed track and the total charge of the event must be zero. The

track which is identified as either an electron or a muon is the tag track. The remaining track is required to be within the acceptance of the DIRC for particle identification and to be identified as a kaon. Furthermore, the signal track must be within 1.0 radians of a well reconstructed π^0 in the CM frame. The π^0 must be reconstructed from two separate EMC deposits that both satisfy quality cuts designed to remove noisy channels and have a χ^2 probability from a constrained mass fit of the two photons which is consistent with being a π^0. To reject non-τ backgrounds, the event shape is used. The events are required to have a thrust greater than 0.9 and the ratio of the $2^{\rm nd}$ to $0^{\rm th}$ Fox-Wolfman moment is required to be greater than 0.5. Moreover, the event must have a total missing momentum of 0.5GeV or more to reduce contamination from Bhabhas and $e^+e^- \rightarrow q\bar{q}$ backgrounds. Contamination from Bhabha events is further reduced by rejecting events if both of the charged tracks satisfy an electron identification algorithm. The final selection efficiency is $2.250 \pm 0.008\%$ with 78112 ± 280 data events selected and $37,610 \pm 159$ background MC events selected. Using equation 3, the preliminary branching fraction is determined to be $(4.39 \pm 0.03 \pm 0.21) \times 10^{-3}$ where the uncertainties are statistical and systematic respectively.

The invariant mass distribution of the selected $K^{\pm}\pi^0$ can be seen in figure 3.

A summary of the systematic uncertainties is shown in table 4. These systematic uncertainties include: the luminosity and cross section determined with KK2F; the particle identification uncertainty; the tracking efficiency; the π^0 efficiency and MC-data correction determined from control samples; the MC statistical uncertainty for signal and background; and the uncertainty of τ background determined from the PDG branching fraction uncertainties.

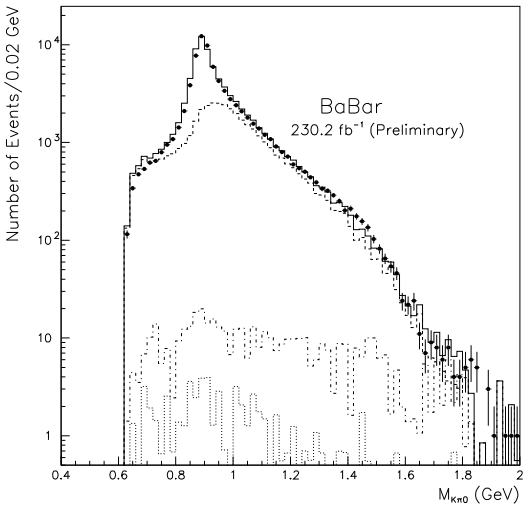

Figure 3. The $\tau \rightarrow K\pi^0\nu$ invariant mass distribution. The dots are the data; the solid line histogram is the signal MC; the dashed line histogram is the τ backgrounds; the dash-dotted line histogram is the $q\bar{q}$ MC; and the dotted line histogram is the $\mu\mu$ MC. The MC samples have been normalized to the luminosity and measured branching fraction of $\tau^- \rightarrow K^{\pm}\pi^0\nu$.

5. Results

The preliminary branching fractions of the $\tau^- \rightarrow h^-h^-h^+\nu$ are measured by means of an efficiency matrix to extract the branching fractions. The $\mathcal{B}(\tau^- \rightarrow \pi^-\pi^-\pi^+\nu\ ex.K^0_S)$ is measured to be $(9.11 \pm 0.01 \pm 0.26) \times 10^{-2}$ a value which is more precise than the previous exclusive measurement directly identifying pions [19]. The $\mathcal{B}(\tau^- \rightarrow K^-\pi^-\pi^+\nu)$ and $\mathcal{B}(\tau^- \rightarrow K^-\pi^-K^+\nu)$ are measured more precisely than the world average; $(2.88 \pm 0.02 \pm 0.11) \times 10^{-3}$ and $(1.371 \pm 0.011 \pm 0.040) \times 10^{-3}$, respectively. The first measurement of the inclusive branching fraction of $\tau^- \rightarrow K^-K^-K^+\nu$ is determined to be $(1.59 \pm 0.14 \pm 0.11) \times 10^{-5}$, a value consistent with the former upper limit [19].

The branching fraction for $\tau^- \rightarrow \pi^-\phi\nu$ and $\tau^- \rightarrow K^-\phi\nu$ are determined by fitting the K^+K^- invariant mass distribution and then using the corresponding efficiency matrix to account for the cross feed. The first measurement of $\mathcal{B}(\tau^- \rightarrow \pi^-\phi\nu)$ is determined to be $(3.49 \pm 0.55 \pm 0.32) \times 10^{-5}$, while $\mathcal{B}(\tau^- \rightarrow K^-\phi\nu)$

Table 4
The preliminary systematic uncertainties for $\tau \to K^-\pi^0\nu$.

Systematic	e-tag	μ-tag	Combined
$\mathcal{L}\sigma_{e^+e^-\to\tau^+\tau^-}$	2.3%	2.3%	2.3%
PID	2.1%	2.3%	2.2%
Tracking Efficiency	0.6%	0.6%	0.6%
π^0 efficiency	3.3%	3.3%	3.3%
Signal MC Statistical	0.5%	0.6%	0.4%
Background MC Statistical	0.6%	0.6%	0.4%
τ Backgrounds	1.4%	1.4%	1.4%
Total	4.8%	5.0%	4.8%

is measured to be $(3.48 \pm 0.20 \pm 0.26) \times 10^{-5}$, a value consistent with the result by Belle [20]. In addition, the $\tau^- \to K^-\phi\nu$ is consistent with saturating the $\tau^- \to K^-K^-K^+\nu$ decay.

The branching fraction of $\tau^- \to K^-\pi^0\nu$ is measured by means of equation 3 to be $(4.39 \pm 0.03 \pm 0.21) \times 10^{-3}$. This branching fraction is the most precise to date and is consistent with the world average ($\mathcal{B}_{PDG}(\tau^- \to K^-\pi^0\nu) = (4.52 \pm 0.27) \times 10^{-3}$ [11]).

Further studies are being conducted inorder to reduce the systematic uncertainty in both the $\tau^- \to h^-h^-h^+\nu$ and $\tau^- \to K^-\pi^0\nu$ preliminary results before they are finalized.

REFERENCES

1. N. Cabibbo, Phys. Rev. Lett. **10** (1963) 531.
2. E. Gamiz, M. Jamin, A. Pich, J. Prades and F. Schwab, Phys. Rev. Lett. **94** (2005) 011803 [arXiv:hep-ph/0408044].
3. S. Chen, M. Davier, E. Gamiz, A. Hocker, A. Pich and J. Prades, "Strange quark mass from the invariant mass distribution of Eur. Phys. J. C **22** (2001) 31 [arXiv:hep-ph/0105253].
4. K. Maltman and J. Kambor, Phys. Rev. D **64** (2001) 093014 [arXiv:hep-ph/0107187].
5. S. Narison, "On the strange quark mass from e+ e- and tau decay data, and test of the Phys. Lett. B **466** (1999) 345 [arXiv:hep-ph/9905264].
6. K. Maltman, "Problems with extracting m(s) from flavor breaking in hadronic tau Phys. Rev. D **58** (1998) 093015 [arXiv:hep-ph/9804298].
7. G. Lopez Castro and D. A. Lopez Falcon, "VMD description of tau → (omega,Phi) pinu/tau decays and the omega Phi Phys. Rev. D **54** (1996) 4400 [arXiv:hep-ph/9607409].
8. J. Wess and B. Zumino, Phys. Lett. B **37** (1971) 95.
9. R. Decker and E. Mirkes, Phys. Rev. D **47** (1993) 4012 [arXiv:hep-ph/9301203].
10. *BABAR* Collaboration, B. Aubert *et al.*, Nucl. Instr. Meth. A **479**, 1 (2002).
11. W. M. Yao *et al.* [Particle Data Group], J. Phys. G **33** (2006) 1.
12. B. F. L. Ward, S. Jadach and Z. Was, Nucl. Phys. Proc. Suppl. **116** (2003) 73 [arXiv:hep-ph/0211132].
13. S. Jadach, Z. Was, R. Decker and J. H. Kuhn, Comput. Phys. Commun. **76** (1993) 361.
14. E. Barberio and Z. Was, "PHOTOS: A Universal Monte Carlo for QED radiative corrections. Version Comput. Phys. Commun. **79** (1994) 291.
15. S. Agostinelli *et al.* [GEANT4 Collaboration], Nucl. Instrum. Meth. A **506** (2003) 250.
16. D. J. Lange, Nucl. Instrum. Meth. A **462** (2001) 152.
17. T. Sjostrand, Comput. Phys. Commun. **82** (1994) 74.
18. H. Albrecht *et al.* [ARGUS Collaboration], Phys. Lett. B **241** (1990) 278.
19. R. A. Briere *et al.* [CLEO Collabora-

tion], Phys. Rev. Lett. **90** (2003) 181802 [arXiv:hep-ex/0302028].
20. [Belle Collaboration], arXiv:hep-ex/0608026.